Journal of Materials Chemistry

www.rsc.org/materials

Volume 20 | Number 2 | 14 January 2010 | Pages 197–400

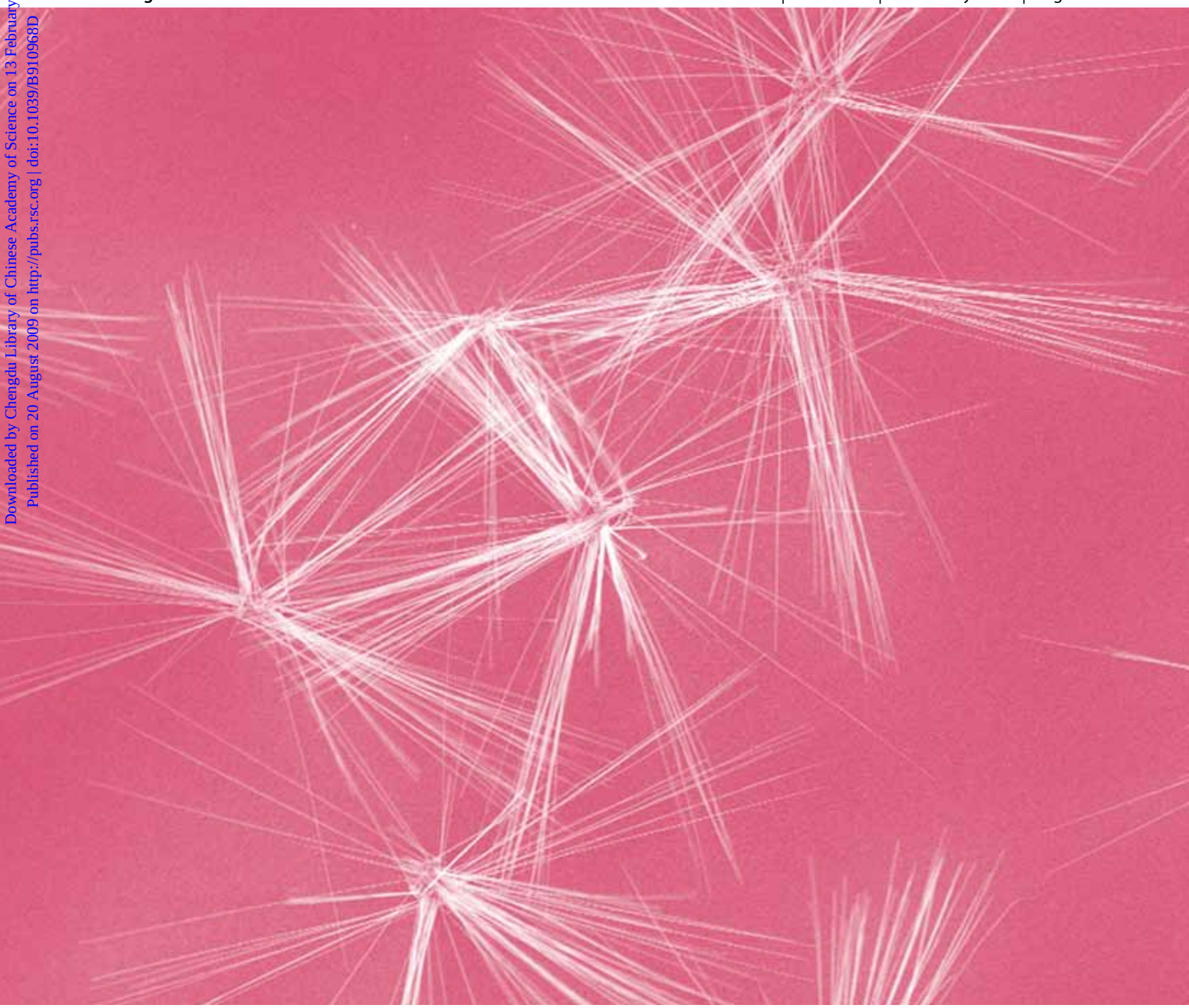

ISSN 0959-9428

RSC Publishing

FEATURE ARTICLE
Andrew L. Schmitt *et al.*
Synthesis and applications of metal silicide nanowires

COMMUNICATION
Nasir M. Ahmad *et al.*
Stable photo-reversible surface energy switching with azobenzene polyelectrolyte mutilayers

0959-9428(2010)20:2;1-9

Synthesis and applications of metal silicide nanowires

Andrew L. Schmitt, Jeremy M. Higgins, Jeannine R. Szczech and Song Jin*

Received 4th June 2009, Accepted 23rd July 2009
First published as an Advance Article on the web 20th August 2009
DOI: 10.1039/b910968d

Transition metal silicides represent an extremely broad set of refractory materials that are currently employed for many applications including CMOS devices, thin film coatings, bulk structural components, electrical heating elements, photovoltaics, and thermoelectrics. Many of these applications may be improved by making 1-dimensional nanomaterials. Chemical synthesis of silicide nanowires is more complicated compared to other classes of nanomaterials due to the complex phase behaviour between metals and silicon and the complex stoichiometries and structures of their resulting compounds. Recently, several synthetic strategies have been developed to overcome this challenge resulting in increasing reports of silicide nanowires in the literature. These strategies are highlighted in this feature article, along with future synthetic challenges and a review of the applications emerging from current silicide nanowires.

Introduction

Metal silicides, the family of refractory, intermetallic compounds between metals and silicon, have diverse physical properties that are both very useful and fundamentally significant. The metallic silicides[1,2] such as NiSi, $CoSi_2$, and $TiSi_2$ provide ohmic contact,[3] interconnect, and gate materials[4] to CMOS microelectronic transistors. Semiconducting silicides[5] have been extensively investigated for silicon-based optoelectronics[6] such as LEDs[7] and IR detectors.[8] The narrow bandgap semiconducting silicides, in particular $CrSi_2$, β-$FeSi_2$, $MnSi_{1.8}$, and $ReSi_{1.75}$, have been targeted and used (β-$FeSi_2$) for robust, stable, and inexpensive thermoelectric materials,[5,9] and have shown promise for photovoltaic[10,11] applications.

University of Wisconsin-Madison, 1101 University Ave., Madison, Wisconsin, 53706, USA. E-mail: jin@chem.wisc.edu; Fax: +1 608 262 0453; Tel: +1 608 262 1562

In addition to finding numerous technological applications, metal silicides have fascinated physicists for over 70 years and continue turning up surprises at the frontiers of theoretical and experimental condensed matter physics. The so-called *B*20 metal monosilicides (MSi, M = iron (Fe), cobalt (Co), manganese (Mn)) are a group of highly correlated electron materials.[12,13] For example, FeSi is the only known transition metal Kondo insulator,[12] a class of heavy-electron compounds exhibiting Kondo lattice behavior at room temperature but having an insulating ground state with a small energy gap. MnSi, long thought of as a classical itinerant ferromagnet and the poster child of metal physics, has recently been discovered to have a quantum critical phase transition[16] and has been observed to exhibit non-Fermi liquid behavior.[17] These monosilicides and their alloys, $Fe_{1-x-y}Co_xMn_ySi$ ($0 < x, y < 1$) also display a myriad of magnetic behaviours, including unusual helical magnetic ordering,[18–20] and even more exotic Skyrmion magnetic phases.[21,22] Furthermore, $Fe_xCo_{1-x}Si$ alloys were recently discovered to be magnetic semiconductors,[23,24] bringing exciting

Andrew Schmitt

Andrew Schmitt received his BA from DePauw University in 2004 and his PhD in 2009 working in the Song Jin research group at the University of Wisconsin-Madison. He won a Materials Research Society Graduate Student Award in 2008 for his thesis work on the synthesis and properties of silicide nanowires. He is starting as a post-doctoral research associate in the same department this fall.

Jeremy Higgins

Jeremy Higgins received his BS from the University of Pittsburgh in 2005 and is a 5th year graduate student in the Song Jin research group. As a Merck Graduate Fellow, he is studying the mechanism of silicide nanowire growth with special emphasis on nanowires for use in thermoelectric applications. His work was recently acknowledged through a UW Madison Energy Hub conference poster award.

prospects of CMOS compatible silicon-based[25] spintronics, a growing field that seeks to exploit the spin properties instead of or in addition to the charge degree of freedom in electronic and photonic devices.[26]

Transition metal silicides fall into a general class of solid state compounds referred to as intermetallics. Intermetallic compounds, composed of at least two metallic elements and optional non-metal components, often have complicated crystal structures. Because of this they are increasingly finding potential applications in a variety of fields, for example, the use of Heussler alloys in spintronics, Nowotny chimney ladder phases in thermoelectrics, and superalloys in structural materials. Structure-property relationships in such compounds are often quite interesting and extremely doping dependent.

New physical phenomena and interesting applications often arise from the reduction of material dimensions to nanoscale.[27,28] During the nanotechnology revolution of the past decade, 1-dimensional (1-D) nanowire (NW) materials[28–33] have enjoyed prominent attention and success. Single-crystalline NWs can be chemically synthesized from the bottom-up with precisely controlled structures, diameters, lengths, chemical compositions and doping/electronic properties using a variety of methods including the nanocluster catalyzed vapour-liquid-solid (VLS)[34] growth process, the most common method for 1-D nanostructure synthesis. These 1-D nanomaterials exhibit diverse device behaviour enabling the successful demonstration of many electronic, photonic, and other functional devices[35] following the bottom-up paradigm of nanotechnology.[36]

Efforts thus far have concentrated on semiconductor channel materials, but metallic contact and gate materials are equally important for continued scaling of CMOS devices.[37] NWs of CMOS compatible metallic silicides having low resistivity and suitable work functions, such as nickel silicides,[4,38] would serve as superior interconnect and gate contacts for nanoelectronic architectures. High quality single crystal semiconducting NWs, such as the half-metallic $Fe_{1-x}Co_xSi$ alloys, will lay the nanomaterials foundation for the exploration of many technologically relevant fields including silicon-based spintronic nanodevices. Since correlations are intimately influenced by length scales and symmetry[12,13] reducing size and dimensionality in the monosilicides and their alloys could lead to interesting new physical phenomena that theoretical physicists have not yet considered. Semiconducting silicides are also known for being robust and inexpensive thermoelectric materials. The most notable are $MnSi_{1.8}$[39,40] and $ReSi_{1.75}$[41,42] with reported figure of merit (ZT) values up to 0.7 and 0.8 in the bulk, respectively. These silicides, along with others such as Ru_2Si_3 and their alloys,[43] belong to defect structure types which can have quite large unit cells; one example, the "Nowotny chimney ladder" phases, have tetragonal structures which can have one lattice constant as large as tens of nanometers.[44–46] It has been predicted[47] and experimentally confirmed[48–51] that dimensional reduction of semiconductors enhances ZT relative to the bulk values due to surface phonon scattering and/or quantum confinement.

Due to their interesting properties and potential applications, we initiated a research program in 2005 to develop free-standing silicide NWs, that to date include FeSi,[52] CoSi,[53] $Fe_{1-x}Co_xSi$,[54] $MnSi_{1.8}$,[55] $CrSi_2$,[56] Ni_2Si,[57] and Ni_3Si.[58] The rational synthesis of NWs from the vapour phase has two fundamental challenges:[28,30,59] 1) delivery of source materials and 2) anisotropic crystal growth to form 1-D nanostructures. Free-standing transition metal silicide nanowire synthesis has been primarily limited by the lack of a general growth scheme such as in VLS grown semiconducting NWs (group IV elements and normal valence compounds such as the II–VI and III–V compounds) that exhibit simple phase behaviour with low melting eutectics (Fig. 1a) that serve as a VLS catalytic system. General and rational chemical synthesis of silicide nanomaterials is challenging, due in part to the multiple stoichiometries and complex phase behaviour exhibited by many silicide compounds.[60] For instance, there are six known iron silicide intermetallic compounds (Fe_3Si, Fe_2Si, Fe_5Si_3, FeSi, α-$FeSi_2$, β-$FeSi_2$) only three of which are stable at room temperature (Fig. 1b).[60] In such complicated materials systems careful control over synthesized phases can be quite difficult. In the last five years, several techniques have been developed for the synthesis of free-standing silicide NWs by ourselves and many other researchers, which can be conveniently categorized into four groups: silicidation of silicon (Si) NWs,

Jeannine Szczech

Jeannine Szczech studied chemistry at the University of Wisonsin-Madison, graduating with a Bachelor of Science degree in 2005. She is currently in her fifth year of studies in the Jin research group, working towards a PhD in Materials Chemistry. Her research focuses on the synthesis and characterization of nanoscale materials with applications in thermoelectric and electrochemical devices.

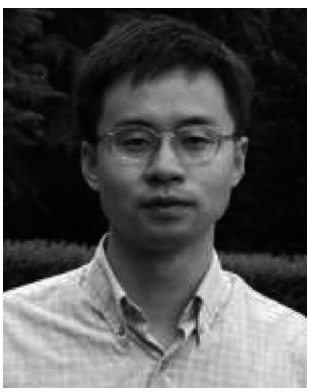

Song Jin

Song Jin received his BS from Peking University in 1997 and his PhD from Cornell University in 2002. He has been an assistant professor of chemistry at the University of Wisconsin-Madison since 2004. He is interested in the chemistry and physics of nanoscale materials and studies metal silicide nanowires, metal chalcogenide nanomaterials, their fundamental formation mechanisms, their novel physical properties and applications in photovoltaic and thermoelectric energy conversion, nanospintronics, and nanomedicine.

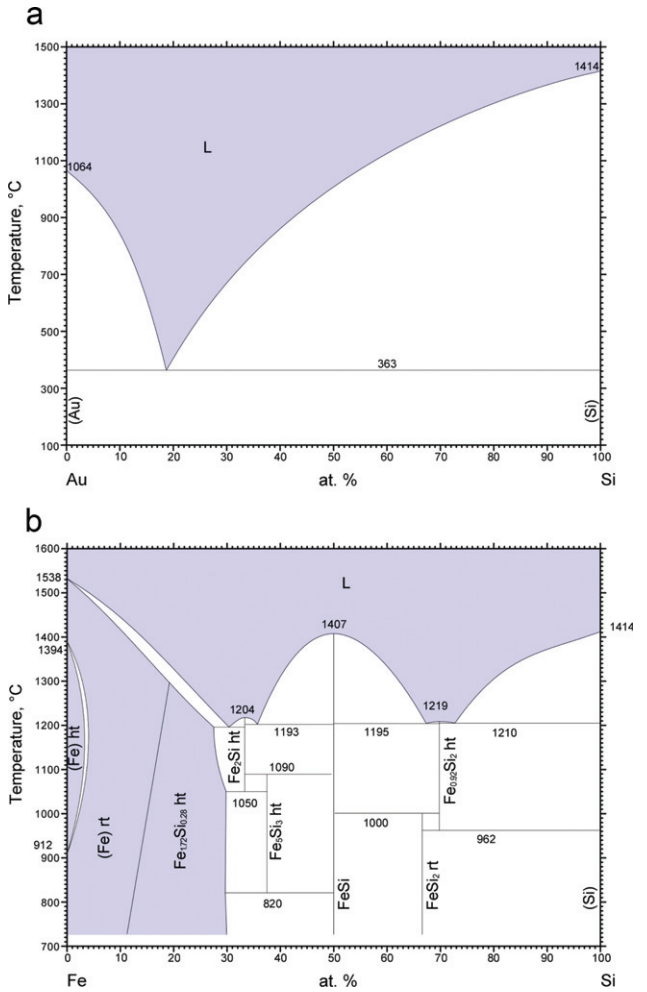

Fig. 1 Binary phase diagrams between a) Au–Si[14] and b) Fe–Si.[15] Reprinted with permission of ASM International (r). All rights reserved. www.asminternational.org

decomposition of silicon on metal thin films, reaction of metals with silicon substrates, and deposition of both metal and silicon *via* chemical vapour deposition (CVD) or chemical vapour transport (CVT).

Today of the eight transition metals that been reported to form silicide NWs, four have more than one reported NW phase (Table 1) in the NW literature. Other examples of solvothermal nanorods[61] and self-assembled epitaxial silicide NWs,[63,64,65] mostly of rare earth silicides on vicinal silicon surfaces, do exist; but, these silicide nanomaterials are distinctively different from the free-standing silicide NWs and not the subject of this feature article. Herein we review the general approaches to the rational chemical synthesis, in a comprehensive manner, of metal silicide nanowires and discuss their current and potential future applications.

Growth techniques

Silicidation of silicon nanowires

Lieber and co-workers reported what was perhaps the first report of transition metal silicide NWs (Fig. 2a).[62] A Si NW backbone, formed using a standard Au nanoparticle mediated VLS process, was covered with a thermally evaporated Ni thin film. Subsequent annealing in forming gas produced single-crystalline NiSi NWs *via* solid state reaction. Furthermore, epitaxial heterojunctions of NiSi and Si were demonstrated allowing the integration of high performance nanowire transistors beyond the lithographic limit. The main challenges in silicide NW formation, material delivery and 1-D anisotropic growth, were overcome independently using this methodology. This work was easily extended to other metals such as Fe to form FeSi, α-$FeSi_2$, and β-$FeSi_2$ NWs[66] and platinum (Pt) resulting in PtSi NWs.[67] However, the nanowires produced in these latter cases were not single crystals.

Other researchers have focused on the *in situ* observation of the silicidation process using transmission electron microscopy (TEM).[68,69] In these experiments VLS grown Si NWs are drop-cast with transition metal nanowires, nickel[68] or cobalt,[69] onto TEM grids in high enough concentration to guarantee direct contact between two different nanostructures (Fig. 2b). For the case of nickel (Ni), which is an extremely fast diffusing species in silicon (0.6 μm/s at 400 °C),[70] Ni atoms "dissolve" into the Si NW at the rapid rate of 1 μm/min. This results in a saturated Ni–Si solid solution until NiSi crystals nucleate at the NW ends. The Si NW is then converted to NiSi one atomic plane at a time until the entire wire becomes fully silicided. Furthermore, highly strained (12%) single-crystalline Si segments can be formed between growing NiSi crystals. In the case of *in situ* silicidation of Si NWs by Co, the phase first nucleated was highly temperature dependent. At low temperature (700 °C) CoSi nucleated while higher temperature (800 °C) led to $CoSi_2$ nucleation. These phases each showed different MSi/Si interfacial behaviour and radically different axial growth rates. Though likely low throughput as a synthetic method, silicidation of Si NWs is an excellent way to directly observe the silicide nucleation process and may be important in understanding the growth mechanisms employed in other MSi NW synthesis schemes. It is also an excellent method to produce MSi/Si heterostructures.

The stoichiometry of silicided NWs could likely be controlled by carefully managing the quantity of evaporated metal; however, certain phases will probably be unobtainable through this technique due to the kinetics of the diffusion process, as is true in thin film and bulk diffusion couples. Such diffusion couples between metals and silicon have been widely studied[1,2,71] and the phases formed can often be predicted by empirical rules such as the so-called "first phase rule".[72] The rule, based on a combination of thermodynamic and kinetic considerations, states that the transition metal silicide formed in a binary diffusion couple is the highest melting temperature congruently melting phase nearest the lowest melting temperature eutectic point in the binary phase diagram.[72] However, it does not appear this rule holds well in the case of diffusion based silicide NW formation as Ni_2Si and Co_2Si are the predicted first phases in the careful *in situ* studies, but NiSi and CoSi seem to be the first phases formed. In the case of evaporated metal diffusing into Si NWs FeSi is the predicted first phase which is observed, but Pt_2Si is the predicted phase while PtSi is actually observed. Predicted phases based on this rule for silicide NW formation are italicized in Table 1, along with phases observed thus far in the nanowire literature (bold) for comparison.

Table 1 Periodic table of the transition metal silicide phases[a]

IA	IIA	IIIB	IVB	VB	VIB	VIIB	VIII	VIII	VIII	IB	IIB
H_4Si											
$Li_{15}Si_4$ Li_2Si											
NaSi $NaSi_2$	Mg_2Si										
KSi KSi_6	Ca_2Si Ca_5Si_3 CaSi $CaSi_2$	Sc_5Si_3 ScSi Sc_2Si_3 Sc_3Si_5	Ti_3Si **Ti_5Si_3** Ti_5Si_4 **TiSi** ***$TiSi_2$***	V_3Si V_2Si V_5Si_3 *VSi_2*	Cr_3Si Cr_5Si_3 CrSi ***$CrSi_2$***	Mn_4Si Mn_3Si Mn_5Si_2 *Mn_5Si_3* MnSi **$MnSi_{2-x}$**	Fe_3Si **(Fe_5Si_3)** ***FeSi*** **$FeSi_2$**	**(Co_3Si)** ***Co_2Si*** **CoSi** Co_2Si_3 $CoSi_2$	**Ni_3Si** ***Ni_2Si*** **$Ni_{31}Si_{12}$** **Ni_3Si_2** **NiSi** **$NiSi_2$**	Cu_3Si $Cu_{15}Si_4$ Cu_5Si	
RbSi $RbSi_6$	Sr_5Si_3 SrSi $SrSi_2$	Y_5Si_3 Y_5Si_4 YSi Y_3Si_5 Y_2Si_3 YSi_2	Zr_3Si Zr_2Si Zr_5Si_3 Zr_3Si_2 Zr_6Si_3 ZrSi $ZrSi_2$	Nb_4Si Nb_3Si Nb_5Si *$NbSi_2$*	Mo_3Si Mo_5Si_3 Mo_3Si_2 *$MoSi_2$*	Tc_4Si Tc_3Si Tc_5Si_3 TcSi Tc_4Si_7	Ru_2Si Ru_5Si_3 Ru_4Si_3 RuSi Ru_2Si_3	Rh_2Si Rh_5Si_3 Rh_3Si_2 RhSi Rh_4Si_5 Rh_3Si_4	Pd_5Si Pd_4Si Pd_3Si *Pd_2Si* PdSi		
CsSi $CsSi_3$	Ba_2Si Ba_5Si_3 BaSi $BaSi_2$	La_5Si_3 La_3Si_2 La_5Si_4 LaSi $LaSi_2$	Hf_2Si Hf_5Si_3 Hf_3Si_2 Hf_5Si_4 *HfSi* $HfSi_2$	Ta_3Si Ta_2Si Ta_5Si_3 ***$TaSi_2$***	W_3Si W_5Si_3 *WSi_2*	Re_3Si Re_5Si_3 ReSi *$ReSi_{1.75}$*	OsSi $OsSi_2$ $OsSi_3$	Ir_3Si Ir_2Si Ir_3Si_2 IrSi $IrSi_3$	Pt_3Si $Pt_{12}Si_5$ *Pt_2Si* Pt_6Si_5 **PtSi**		

[a] Bold phases have been observed in nanowires, italicized phases are predicted 1st phase rule phases, and metastable nanowire phases are in parentheses.

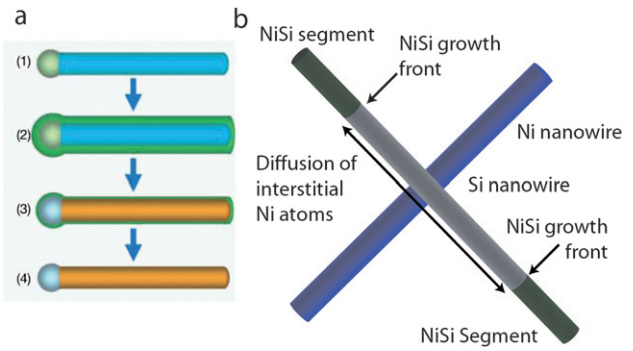

Fig. 2 Preparation of NiSi NWs by silicidation. a1) Si NWs (blue) are synthesized *via* VLS and a2) coated with Ni metal (green), a3) reacted at 550 °C to form NiSi nanowires (orange). a4) Extra Ni metal is etched away leaving single crystalline NiSi NWs.[62] b) Preparation of NiSi NWs by point contact silicidation to form NiSi–Si NW heterostructures.

Delivery of silicon to metal films

In lieu of using a Si NW backbone, the first challenge of silicide NW growth (source material delivery) must be addressed. One way to accomplish this for binary systems is to deliver either the Si or the metal and use the other as a substrate. This approach can be advantageous as fewer gas phase species simplifies the experiments. A scheme for the delivery of Si using silane precursors was easily adopted from the wealth of reports detailing CVD synthesis of silicon NWs.[73,74] Synthetic strategies emerged for the decomposition of SiH_4 on metal thin films or through using vapour phase elemental silicon through evaporation or sputtering resulting in free-standing silicide NWs.[70,75–80] Interestingly, to date this strategy has only been reported for NWs of nickel silicides: $NiSi_2$,[79] NiSi,[76,77,80] Ni_2Si,[70,79,80] Ni_3Si_2,[78] $Ni_{31}Si_{12}$,[81] and Ni_3Si[75] (all of the room temperature stable nickel silicide phases). Even with reports dating back to 2004,[79] little significant work has been done in this time to uncover the mechanism behind this particular growth method. A possible reason that this strategy has been reported only for nickel silicides is the extremely fast diffusivity of Ni in Si.[70] Many transition metals can be used to catalyze Si NW growth *via* either the VLS mechanism[60] or the vapour-solid-solid (VSS) mechanism.[74] Ni itself is actually one of the earliest reported VLS catalysts for Si NW growth.[82] Either nanocrystals of $NiSi_2$ phase (through which Si is the dominant diffuser) or low temperatures must be employed to prevent the dissolution of Ni catalyst into the silicon material before wire formation occurs. If higher temperatures and a practically limitless metal source (metal substrate or thick film) are used, nickel silicide NWs are observed.

The growth of Ni_2Si NWs on a Ni thin film (Fig. 3) is one of the more complete analyses of this silicide NW synthesis method.[70] Generally, silane decomposes onto the Ni surface leading to the growth and elongation of Ni_2Si nanocrystals. These nanocrystals continue to elongate decreasing the available area for Ni diffusion along the surface. Eventually the Ni incorporation rate through diffusion equals the rate of silane decomposition (or Si addition), resulting in the formation and propagation of thin, untapered Ni_2Si NWs. Kang and co-workers have also showed that Ni_xO layers can be used to help control the initial stages of 1-D growth by serving as a diffusion barrier for Ni.[80]

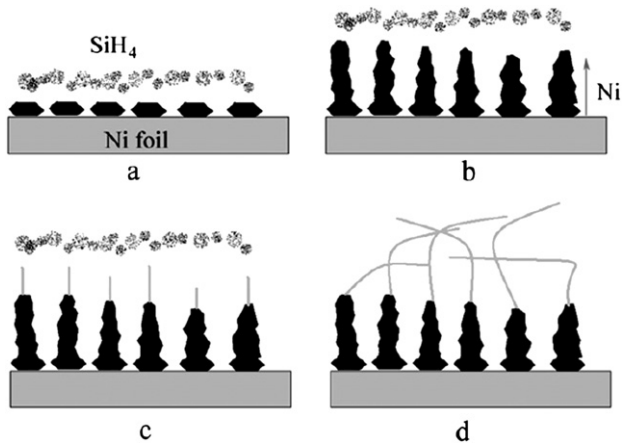

Fig. 3 Preparation of Ni_2Si NWs using silane gas precursor and Ni foil. (a) Ni diffusion is faster than silane decomposition, creating nanoparticles on the surface of the metal film. (b) As more Si decomposes, Ni metal from the substrate has to diffuse further into the crystalline material, creating an elongated structure. (c) The rates of metal diffusion and silane decomposition are comparable and single crystalline NWs form. (d) NWs with constant diameter are propagated during growth.[70]

In spite of its simplicity, only nickel silicides have been produced using this technique, serving as a strong indicator of the role of diffusion in this process. Other silicides might be formed using this method if higher temperatures are used to activate diffusion, but alternative silicon precursors with elevated decomposition temperatures would be required.

Reactions of transition metal sources with silicon substrates

One could react transition metal species directly with silicon substrates to make silicide NWs. While a variety of simple organometallic complexes are known to decompose to deliver metal,[83] to date only pure metal vapours and anhydrous metal halides have been used to yield free-standing metal silicide NWs.

Metal vapour

Chueh and co-workers initially reported the synthesis of short (0.2–2 μm) $TaSi_2$ NWs *via* annealing silicon substrates with $FeSi_2$ thin films or $FeSi_2$ nanodots on their surface in a tantalum (Ta) atmosphere.[84] It was believed that Si atoms segregate from either the $FeSi_2$ thin film or nanodots to form a nanoparticulate Si base. Ta atoms adsorb onto the surface of either the $FeSi_2$ thin films or nanodots and react with Si diffusing through the substrate to form $TaSi_2$ nanocrystals. Because of the high temperatures and low pressures used, certain facets are favoured and one-dimensional growth is observed. The use of a different silicide film can increase the aspect ratio of generated NWs;[85] however, in all cases the metal impurity from the starting silicide thin film (or nanodots) is found in the final product, accounting for as much as 10% of the total elemental content. Other work reported by the same group provides insight; annealing similar $FeSi_2$ substrates in the absence of Ta vapour but under higher temperature conditions produces silicon NWs.[86] This result is not surprising considering the well known use of Fe and its metal silicides as VLS or VSS catalysts for the growth of Si NWs; Fe was one of the first VLS catalysts reported.[73,82] These metal silicide particles likely served as both the 1-D catalyst and path for incorporation of Si from the substrate. Considering the work done on silicidation of Si nanowires, it is probable that the $TaSi_2$ NWs were formed by the silicidation of silicon nanowires either as they are formed or shortly thereafter. This method of silicide NW growth requires high temperatures (950 °C), long reaction times (16 h), and yields impure products, but it is the only method reported to date of $TaSi_2$ NW production.

Metal halides

The application of anhydrous metal halides as the transition metal source for reaction with Si substrates has proven to be a general and popular method to grow silicide NWs. Ouyang and co-workers reported this technique as a facile way to produce FeSi nanowires using $FeCl_3$.[87] Varadwaj *et al.* further used a two-zone furnace to give better control of the metal halide vapour pressure.[88] Typically, a halide precursor is vaporized in the upstream zone of a furnace, kept around 500 °C, and the substrate is held at 900 °C during the course of the reaction. Interestingly, by using substrates other than Si, metal rich phases can be favoured (Si powder or a Si substrate is still required for NW growth).[88] Using this approach, NWs of FeSi,[87] $TiSi_2$,[89] Ti_5Si_3,[90] Fe_5Si_3,[88] CoSi,[91] Co_2Si,[91] $CrSi_2$,[92] and $Fe_{11-x}Co_xSi$[93] have been reported. Although no convincing mechanism has been reported, vapour-solid (VS) mechanisms are usually proposed based largely on the delicate dependence of halide supersaturation on the resultant silicide morphology and phase. At lower pressures, the halides become more volatile and metal rich phases are preferred. Metal chlorides are well known to react with Si to produce $SiCl_4$, MSi_x, and/or Cl_2. $SiCl_4$ is likely providing vapour-phase Si that could decompose to form elemental silicon or silicide, releasing more Cl_2 into the vapour phase. $SiCl_4$ is widely used to grow silicon NWs at such high temperatures.

One possible mechanistic explanation, usually discounted by researchers, is the growth of Si NWs catalyzed by *in situ* grown metal silicide nanoparticles followed by eventual silicidation of these NWs that could be carried out by reaction with metal deposited on their surfaces or diffusing from the substrate. The lack of a catalyst particle tip does not rule out particle catalysts as being responsible for 1-D growth as it possible to have a surface bound catalyst particle or a particle that is eventually incorporated into the wire itself, as is seen, for example, in the case of lead (Pb) catalyzed lead chalcogenide NWs.[94] Thus far the delivery of transition metals to a silicon surface *via* a metal halide has proven to be a very versatile and general method to produce TMSi NWs of both slow and intermediate diffusing TM species.

Simultaneous metal and silicon delivery

Simultaneous delivery of silicon and transition metal source material to a substrate to grow metal silicide NWs has been achieved using two different techniques: chemical vapour transport (CVT) and chemical vapour deposition (CVD).

Chemical vapour transport (CVT)

CVT, a classical crystal growth method, takes advantage of the reversible thermodynamic reaction between two chemical

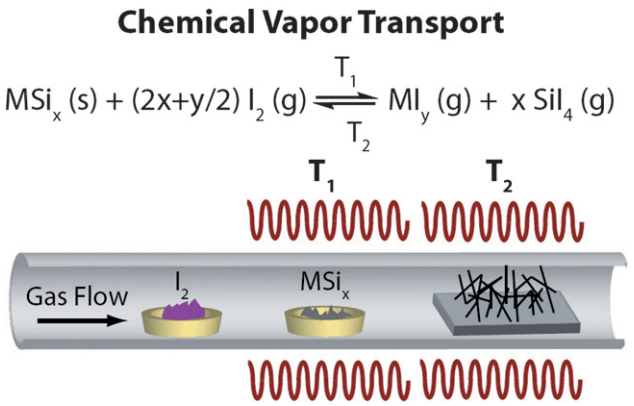

Fig. 4 Synthesis of metal silicide NWs using chemical vapour transport (CVT). Silicides undergo reversible reaction with I_2 at T_1 to form *in situ* gas phase products. At T_2 gas phase components undergo the reverse reaction to form silicide NWs.

species, a source material and a transport agent, to produce gas-phase precursors *in situ*. The intermediates provide the elements needed to synthesize the desired phase, as shown in Fig. 4. This technique has been widely used to synthesize single crystals of many of the transition metal silicides.[95] However, one-dimensional NW growth may be obtained by altering the process for kinetically-favoured growth of 1-D morphologies.

We have demonstrated the synthesis of three distinct single-crystalline silicide NW phases *via* continuous-flow CVT using iodine (I_2) as the transport agent.[56–58] In each case, growth occurred on Si/SiO_2 substrates, sometimes requiring a dilute metal salt solution of $Ni(NO_3)_2$ on the surface. Hexagonally-faceted $CrSi_2$ NWs with lengths up to a few hundred microns were synthesized using powdered $CrSi_2$ as the source material.[56] NWs of the δ-Ni_2Si[57] and β-Ni_3Si[58] phases were also synthesized using Ni_2Si and $TiSi_2$ as source materials respectively. For both $CrSi_2$ and δ-Ni_2Si, the product stoichiometry was identical to the stoichiometry present in the source material. Interestingly, the β-Ni_3Si phase was obtained when $TiSi_2$ was used as a source material; it appears that the Ni in this case was supplied from the $Ni(NO_3)_2$ solution, with the Si emanating from the generated SiI_4. Elemental analysis of the β-Ni_3Si NWs revealed that no titanium (Ti) was incorporated into the NWs. Further impurity doping by I_2 was not detected by energy dispersive spectroscopy (EDS) for any of the above phases.

Although the exact growth mechanism has not been determined for CVT grown silicide NWs, the lack of a visible catalyst tip combined with the necessity of the metal salt solution has been used to rule out VLS-type growth and typically vapour-solid or metal-assisted NW growth is cited. While among the synthetic free-standing nanowire literature there have been no confirmed reports of VLS catalyzed transition metal silicide nanowires the potential for *in situ* silicidation of silicon NWs remains.

Chemical vapour deposition (CVD)

CVD using single source precursors. The use of single source precursors (SSP), inorganic complexes containing the transition metal and silicon atoms necessary for silicide formation, as the vapour phase source material has been shown to be one of the most successful and versatile transition metal silicide NW synthesis techniques to date. SSPs have been used in MOCVD to obtain transition metal silicide thin films.[83] Compared with conventional multisource metal organic CVD, the SSP approach allows simpler and safer experimental setups due to the elimination of highly hazardous liquid precursors ($Fe(CO)_5$ typically for Fe and $SiCl_4$ for Si), easier and precise control over stoichiometry, and higher quality material growth,[83,96] *i.e.* FeSi and CoSi thin films have been deposited by the pyrolysis of *cis*-$Fe(CO)_4(SiCl_3)_2$[97] and $Co(CO)_4SiCl_3$.[98] By selecting simple inorganic molecules containing metal and silicon that vaporize and decompose through well known pathways, precise control of the product stoichiometry and reproducible growth of NWs is possible (Fig. 5).

We first demonstrated this approach by using *trans*-$Fe(CO)_4(SiCl_3)_2$ (the *cis* isomer is converted to *trans* at higher temperatures) to synthesize FeSi NWs.[52] This compound can be readily synthesized by reacting $Fe_3(CO)_{12}$ with excess $SiHCl_3$ in an inert atmosphere at 120 °C for 2 days and readily decomposes into FeSi in the gas phase at elevated temperatures (Fig. 5). High quality FeSi NWs can be synthesized using the CVD deposition of this precursor at 200 Torr and 750 °C when Si substrates are prepared with a thin (1–2 nm) silicon oxide layer.[53] The dependence of this oxide layer was shown through patterning experiments,[108] which also serves as a simple method to define the locations of silicide NW growth without the use of catalysts. To date, this general approach (Fig. 5) has been extended to CoSi NWs[53] using $Co(CO)_4SiCl_3$ and $MnSi_{2-x}$ ($MnSi_{1.8}$) NWs[55] using $Mn(CO)_5SiCl_3$. *trans*-$Fe(CO)_4(SiCl_3)_2$ and $Co(CO)_4SiCl_3$ SSP mixtures can themselves form a liquid two-component single source precursor *via* melting point depression. This solution can be conveniently evaporated for vapour phase delivery resulting in

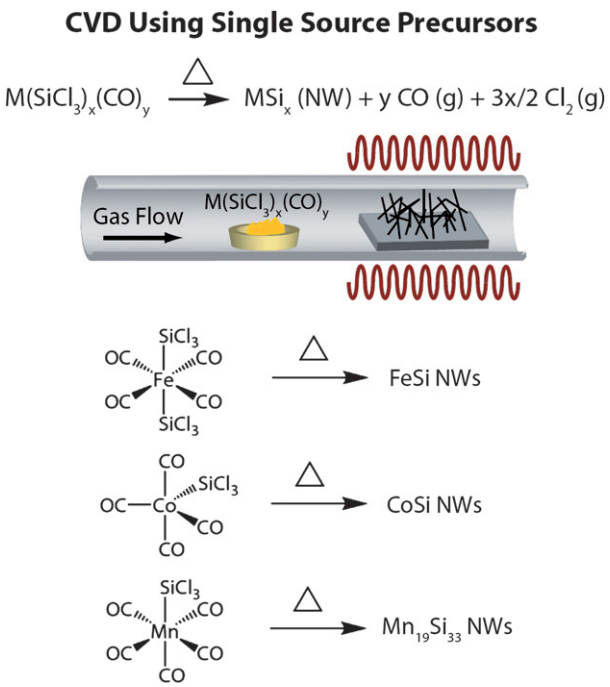

Fig. 5 Synthesis of metal silicide NWs using chemical vapour deposition (CVD) of single source precursors (SSP). Each SSP pyrolyzes to deliver metal silicide material to the growth substrate.

the synthesis of $Fe_{1-x}Co_xSi$ alloy NWs.[54] Such NWs are particularly interesting for spintronic applications as discussed below. Interestingly, the iron silicide and manganese silicide phases formed do not share their stoichiometry with that of the starting precursor. In the case of FeSi NW formation the precursor is known to undergo a reductive elimination to $FeSiCl_2$ upon pyrolysis which may give rise to the resultant NW stoichiometry,[97] but the stoichiometry of the $MnSi_{2-x}$ NWs produced from $Mn(CO)_5SiCl_3$ cannot be similarly rationalized as the pyrolysis behaviour of the precursor is ill characterized. The higher manganese silicides produced using this precursor are an incredibly complex set of incommensurate structures based on elemental sublattices of Mn atoms which form chimneys within which spiralling sublattices of Si atoms lie.[109] These so-called Nowotny chimney ladder phases can have unit cells (under commensurate approximations) of up to 10s of nm.[110] The NWs were determined to be $Mn_{19}Si_{33}$ by elaborate electron diffraction experiments. Such structures, having both complex crystal structures and enhanced nanomorphology, are efficient phonon scatters which improves upon their thermoelectric performance.[111]

Preliminary experiments into the mechanism for this process show that both silicon and metal atom diffusion from the substrate is occurring and may be used to make solid solutions for spintronics, *i.e.* $Fe_{1-x}Co_xSi$, or for doping thermoelectric phases, *i.e.* $MnSi_{2-x}$. Importantly, because the decomposition pathway may produce gas phase silicon, either through direct decomposition or Cl_2 substrate etching, silicidation of VLS grown silicon nanowires should not be ruled out. Although there are many more transition metals (examples include Ru, Re, and Rh) capable of making analogous molecules which are both volatile and contain metal-silicon bonds, many of the early transition metals do not. Such transition metal silicide NW phases of interest are likely accessible only through alternative source material delivery techniques. As new developments occur in metal-silyl complexation chemistry, new SSPs will be developed that allow other stoichiometries and new combinations of transition metals and silicon to be delivered *via* gas phase pyrolysis for NW growth.

Two source CVD. CVD of silicon and metal gas phase sources is the classical way in which to prepare silicide thin films for electronic applications. Typically, silane and metal carbonyls are used at low temperatures (250–450 °C) to produce thin films with controlled stoichiometries. Zhou *et al.* were able to adapt a similar approach to form $TiSi_2$ nanostructures.[106] In these experiments $TiCl_4$ and SiH_4 were co-flowed with H_2 gas to a Si substrate at 675 °C to form orthorhombic $TiSi_2$ nanowires (C54) and 2-D nanonets (C49). The nanonets are composed of hyperbranched $TiSi_2$ nanowires restricted along the [100] and [001] growth directions of the C49 orthorhombic structure. The same authors also showed that by varying the Si:Ti ratio (intermediate between the optimized C54 and C49 structures), nanonets can intersect at 120° angles to form 3-D nanonets.[107] This likely occurs through a hexagonal C40 $TiSi_2$ coating along the axis of intersection. So far, the two source CVD approach has only been successfully applied to the synthesis of titanium silicide NWs. The inherent strength of the dual source approach is the independent control over Si and TM vapour pressures, but this technique has not yet been shown to be general for other metal silicides.

Technique comparison

Many observations and conclusions can be drawn when summarizing across the various growth techniques used to produce the entire array of silicide NWs reported to date (Fig. 6). Diffusion seems to be an important parameter for silicide NW growth, considering that there have been more reports of silicide NW growth from the Ni-Si binary phase diagram than any other. This is likely due to the exceptionally fast diffusion behaviour of nickel in silicon. By simply decomposing silane on Ni metal films using a wide variety of conditions (10–160 Torr, 400–650 °C, 10–60 min growth times, and surface oxidation behaviour (see Table 2)), different parts of the phase diagram can be accessed resulting in NWs of many nickel silicide phases. Ni silicides can also be grown using CVT to give ultra-long wires (up to 3 mm), but require longer reaction times (2 h) and higher temperatures (1000 °C).[57]

Early transition metal silicide nanowires, sometimes called refractory metal silicides, are probably the most difficult to make from the perspective of metal diffusion. Metals such as Ti, vanadium (V), niobium (Nb), Ta, *etc.* are slow diffusing species and form silicides with extremely high melting points. At the time of submission, only TiSi,[105] Ti_5Si_3,[90] $TiSi_2$,[89,106] and $TaSi_2$[84] have been reported. $TaSi_2$ and $TiSi_2$ were synthesized using the reactions of metal vapour with silicide thin films or bare Si substrates, respectively. Ti_5Si_3 NWs were synthesized using the direct reaction of $TiCl_4$ with a silicon substrate. These synthetic procedures require high temperatures, and in the case of $TaSi_2$ extremely long reaction times of up to 16 h yielding only short (1–2 μm) NWs. There are no reported alternatives yet to produce these materials; however, TiSi and $TiSi_2$ nanowires were recently synthesized using a dual source CVD approach.[106] The lack of single source precursors and slow diffusion behaviour of the early transition metal species implies that successful synthesis of silicide NWs of early transition metals will require vapour phase transition metal *and* silicon delivery using either CVD or CVT.

Silicides of the group VIB metals, chromium (Cr), molybdenum (Mo), and tungsten (W), which are also considered refractory, are an interesting intermediate case. So far the only silicide phase synthesized among this group has been $CrSi_2$; NWs of this phase have been produced independently by both CVT and metal halide transport.[56,92,103] The mechanism for growth in these two processes is likely very similar. Metal halide transport evaporates $CrCl_2$ and produces $SiCl_4$, from reaction with the silicon substrate. By delivering $CrSi_2$ *via* I_2 transport agent, CVT produces CrI_2 and SiI_4. These are borne out in the nearly identical morphologies observed in the two cases (Fig. 6). It has yet to be seen whether either of these techniques, or others, can be used to make tungsten or molybdenum silicides, but because of the generally slow diffusion behaviour of these metals, synthesizing such NWs will be difficult using either delivery of a silicon source to a metal substrate or vice versa. For these metals there are no $M(CO)_x(SiCl_3)_y$ analogs because the M–Si bond in such structures is quite weak, but precursors stabilized by cyclopentadienyl or π-arene ligands are known and delivery of such SSPs or independent Si and TM sources *via* CVD may lead to successful NW synthesis.

The late transition metal (except groups IB, IIB) silicides have been explored using both metal halide transport and CVD of single source precursors.[52–55,87,88,91,93,108] In the case of single

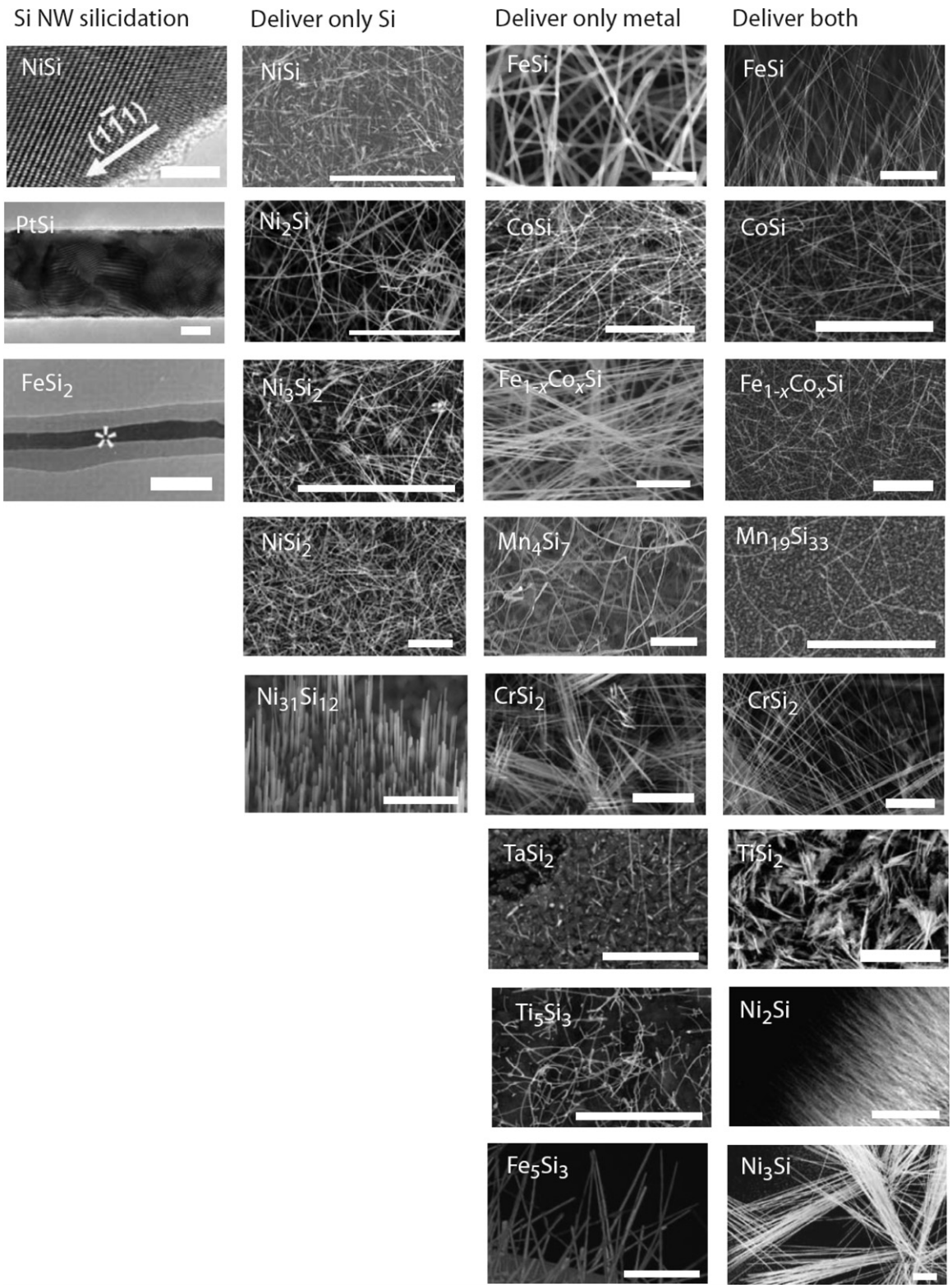

Fig. 6 Morphologies of transition metal silicide nanowires. Images of transition metal nanowires synthesized for four different paradigms. Silicon nanowire silicidation: Si NW silicidation yields NiSi,[68] PtSi,[67] and $FeSi_2$[66] NWs, 1st column TEMs (scale bars 5, 20, and 100 nm, respectively). Silane reactions with metal: delivery of only Si to metal substrates results in NiSi,[77] Ni_2Si,[70] Ni_3Si_2,[78] $NiSi_2$,[100] and $Ni_{31}Si_{12}$[81] NWs, 2nd column SEMs (scale bars are all 5 μm). Metal delivery to silicon: delivery of transition metals using silicon substrates yields FeSi,[87] CoSi,[91] $Fe_{1-x}Co_xSi$,[93] Mn_4Si_7,[104] $CrSi_2$,[92] $TaSi_2$,[85] Ti_5Si_3,[90] and Fe_5Si_3[88] NWs, 3rd column SEMs (FeSi and Mn_4Si_7 scale bar is 1 μm, the rest are 5 μm). Delivery of both metal and silicon: using either CVT or CVD to deliver metal and silicon results in FeSi,[52] CoSi,[53] $Fe_{1-x}Co_xSi$,[54] $Mn_{19}Si_{33}$,[55] $CrSi_2$,[56] $TiSi_2$,[106] Ni_2Si,[57] and Ni_3Si[58] NWs, 4th column SEMs (all scale bars are 5 μm except Ni_2Si which is 200 μm).

Table 2 Comparison of silicide nanowire growth techniques

Scheme	TM source	Si source	Temp. range	Rxn time	Pressure	Length	Phases
Si NW silicidation	TM evaporation	Si NWs	550–700 °C	3–4 h	760 Torr	10–20 μm	$CoSi$,[69] $CoSi_2$,[69] $NiSi$,[62,68,99] $PtSi$,[67] $FeSi$,[66] $FeSi_2$[66]
Si delivery to metal	TM films or foils	SiH_4	400–650 °C	10–60 min	10–160 Torr	2–20 μm	Ni_2Si,[70,79,80] $Ni_{31}Si_{12}$,[81] Ni_3Si_2,[78] $NiSi$,[77,80] $NiSi_2$[100]
TM vapor delivery	TM vapor	Si substrate	850–950 °C	4–16 h	1×10^{-6} Torr	1–10 μm	$TaSi_2$,[84,85] $TiSi_2$[89]
TM halide delivery	TM halides	Si substrate	900–1100 °C	0.5–2 h	500–760 Torr	1–20 μm	$FeSi$,[87,101] Fe_5Si_3,[88] Co_3Si,[102] Co_2Si,[91,102] $CoSi$,[91,101,102] Ti_5Si_3,[90] $CrSi_2$,[92,103] $Fe_{1-x}Co_xSi$,[93] Mn_4Si_7[104]
CVT	TM silicides		900–1000 °C	2–3 h	760 Torr	10 μm to 5 mm	$CrSi_2$,[56] Ni_2Si,[57] Ni_3Si[58]
2-source CVD	TM halides	SiH_4	650–730 °C	15 min	5–760 Torr	2–5 μm	$TiSi$,[105] $TiSi_2$[106,107]
SSP CVD	$M(CO)_x(SiCl_3)_y$		650–750 °C	30 min	100–200 Torr	10–40 μm	$FeSi$,[52,108] $CoSi$,[53] $Fe_{1-x}Co_xSi$,[54] $Mn_{19}Si_{33}$[55]

source precursors, the metal to silicon ratio delivered to the substrate can be built into the molecular structure as a means of gaining more control over the reaction. In metal halide transport similar results can be obtained albeit at much higher temperatures (900–1100 °C, Table 2). Varadwaj *et al.* were able to show that by eliminating substrate diffusion as a silicon source and instead relying on gaseous $SiCl_4$ products, metal rich phases can be favoured.[88] This makes it possible to choose between two phases by changing the substrates. In order to do this using the SSP approach, metal-silicon bonds in the molecules would have to be tuned for bond strength using crystal field theory and molecular design criteria to alter the decomposition products. Fundamental research in this area could yield many more SSP targets for the controllable synthesis of silicide NWs.

Across the board, the mechanism for the anisotropic 1-D growth of silicide NWs is not very clear. Nearly all reports believe silicide NWs were not directly formed *via* a VLS or metal-catalyst driven process regardless of the precursor delivery methods. The strong correlation with metal diffusion behaviours in silicon, the dependence on various oxide of silicide diffusion barriers, and other observations seem to imply that diffusion and reaction is an important consideration. Thus far there have been no confirmed reports of VLS catalyzed transition metal silicide nanowires, but based on the reaction parameters discussed for each process, it seems plausible that silicon NWs are being formed prior to silicidation *via* metal incorporation from diffusion or directly from the gas phase. Further investigation is still needed to elucidate such mechanisms. It should also be noted that for many cases little attention has been paid to the interface between the NW and the growth substrate leaving the possibility of nanoparticle mediated 1-D nucleation from the base an open possibility. We are currently investigating this using TEM of microcleaved samples.

Applications of silicide nanowires

Transition metal silicides, with their diverse physical properties, have been used in a large number of applications. High melting points, excellent chemical stability, and compatibility with silicon processing technology have made them good candidate materials for use in electronics, thermoelectrics, and photovoltaics.[2,5,116,117] Metal silicide nanowires share these positive characteristics and their size may allow them to be useful in potentially improved nanoscale versions of these devices as well as in new roles, such as field emission sources and spintronics. In the following section we briefly review the applications and current device concepts utilizing silicide NWs.

Nanoelectronics

Because of the ubiquity of metal silicides as interconnects and contact electrodes in modern microelectronics,[118] silicide NWs are expected to serve a similar role in nanoelectronic devices. Their low resistivities and compatibility with silicon make them excellent candidates to continue in this role. Notably, ultralong Ni_2Si NWs were made having an extremely low resistivity of 21 μΩcm and were capable of supporting remarkably high failure current densities >108 A/cm^2 (Fig. 7a).[57] The difficulty of selective nanostructure placement for devices serves as a strong barrier against the use of randomly oriented free standing NWs. A number of groups have found a solution through the direct silicidation of silicon nanowires creating so-called intruded silicon contacts.[62,99,112] In this process metal contacts lithographically applied to silicon NWs are used as the metal source to controllably create MSi/Si/MSi heterostructures (Fig. 7b). Careful control of this phenomenon has been applied in the successful fabrication of NiSi NW contacted Si FETs with arbitrary channel length.[99] Indeed such a strategy may be used as an exploration of new types of devices as quantum confined[112] and highly strained[68] silicon segments have also been demonstrated.

Nanoscale field emitters

Another commonly discussed application for metal silicide NWs is their use as nanoscale field emitters (Fig. 7c). Field emission occurs when an electric field between a metallic surface and a ground electrode allows electrons to overcome the work function potential that binds them on the surface of the emitter. The field emission current follows the Fowler-Nordheim relation: $J = (A\beta^2E^2/\Phi)\exp(-B\Phi^{3/2}/\beta E)$ where J is the current density, E is the applied electrical field, Φ is the work function, β is the field enhancement factor, and A and B are constants: 1.56×10^{-10} (AV^{-2}eV) and 6.83×10^3 (eV$^{-3/2}$μm^{-1}) respectively.[119] Field emission devices are useful in wide ranging applications such as flat panel displays, microwave generation devices, and high-powered vacuum microelectronic devices. Since the late 1990s there has been much interest in developing 1-D nanomaterials for field emission due to the enhancement of electric field at the high

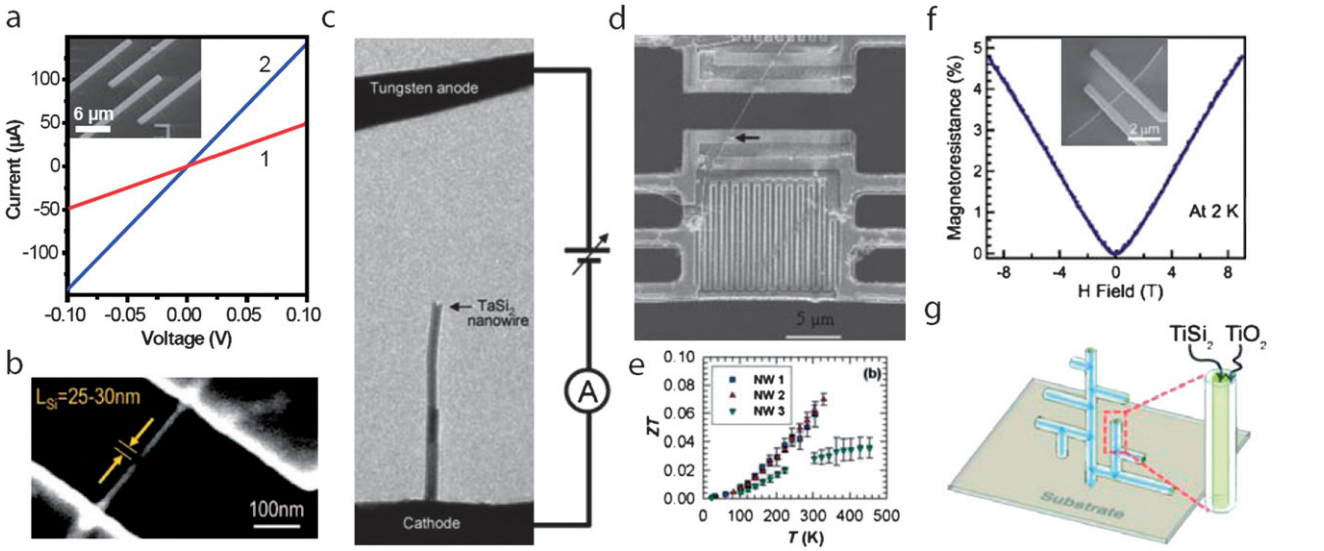

Fig. 7 Applications of transition metal silicide NWs. a) Two-probe (1) and four-probe (2) electrical transport for single Ni_2Si NW.[57] b) Intruded contact NiSi–Si–NiSi quantum dot device.[112] c) Single $TaSi_2$ NW field emission device.[113] d) $CrSi_2$ NW on suspended measurement device to investigate thermoelectric properties, notice open central region available for TEM characterization of NW.[114] e) ZT as a function of temperature for three different $CrSi_2$ NWs.[114] f) Large positive magnetoresistance of $Fe_{1-x}Co_xSi$ NW, inset is example measurement device.[54] g) $TiSi_2$ nanonet–TiO_2 heterostructure for photoelectrocatalytic device.[115]

curvature tips. Thus as the geometric enhancement factor β increases, the voltage required for emission decreases. Because transition metal silicide NWs have low resistivities and work functions, high melting points, high aspect ratios, and well known compatibility with silicon-based microelectronics they have been considered good candidates for future field emission devices. The field emissions of as-grown, free-standing transition metal silicide NWs of a variety of phases have been reported including Ni_2Si,[70] NiSi,[75] $TaSi_2$,[84,85] $TiSi_2$,[89] Ti_5Si_3.[90] Authors regularly report turn-on fields (for current density of 10 μA/cm^2) in the range of 3–4 V/μm and field enhancement factors as high as 4280.[70] Studies on single NW field emitters have also begun in the hopes of pushing current theoretical understanding of the field emission in these nanoscale structures.[113]

Spintronics

As the size of transistors approaches the quantum regime many researchers have begun to consider alternative computing paradigms. Spintronics is an approach which seeks to use the electron's spin degree of freedom in lieu of or in addition to the electron's charge for computation.[26] The long spin relaxation times and well developed process technology of silicon make it an ideal candidate material for devices such as a spin-FET.[120] Such technologies are still in their infancy as the difficulties associated with spin-polarized and pure spin current injection and detection are still being solved. The conductance mismatch problem[121] prohibits the use of conventional ferromagnetic metals as the contacts in a spin-FET due to greatly enhanced interfacial spin scattering, but novel contact materials, such as half-metals and ferromagnetic semiconductors, would overcome this barrier.[26] NWs of the $Fe_{1-x}Co_xSi$ alloys, which contains both half-metallic and ferromagnetic semiconducting members in the bulk phase,[23,122] have been synthesized independently by two different groups, one using single source precursors with $0 < x < 0.44$[54] and one using metal halides with $0 < x < 0.1$.[93] In both preparations, the NWs have been shown to retain bulk-like magnetic and electrical characteristics (Fig. 7f). Although large magnetoresistances have been reported (~10%), there have not been measurements of the spin polarization (P_s) in this material. We are currently working on using point contact Andreev reflection to precisely determine the value of P_s in this interesting system.

Thermoelectrics

The aim of thermoelectricity is the efficient interconversion of thermal and electrical energy using solid state devices. Metal silicides have long been considered a promising group of materials for thermoelectric applications, especially power generation at elevated temperature. The efficiency of a thermoelectric material is judged by the unitless parameter $ZT = S^2\sigma T/(\kappa_L + \kappa_e)$, with S the Seebeck coefficient, σ the electrical conductivity, κ_L the thermal conductivity due to the lattice, κ_e the thermal conductivity due to electrons, and T the average measurement temperature. Recent research in materials development for such applications follows the "electron crystal phonon glass" paradigm,[111] producing materials which strongly scatter phonons but allow efficient electrical transport. The two major strategies for accomplishing this involve using materials with complex crystal structures or nanoscale morphology, both of which lead to relatively small lattice thermal conductivity. Nanowires of $CrSi_2$[56,92] and the Nowotny chimney ladder (NCL) $MnSi_{2-x}$,[55] which are excellent bulk thermoelectric materials, have been successfully synthesized. Further, specific thermoelectric properties of $CrSi_2$ nanowires have been investigated using a specialized technique allowing the measurement of all thermoelectric properties on a single wire in addition to structural characterization *via* TEM which revealed increased phonon-surface scattering with decreasing NW diameter at low temperatures (Fig. 7d,e).[114] Additionally, phonon confinement

will occur more readily in nanostructured materials which with enhanced phonon-surface scattering and complex crystal structures will result in dramatic reduction of thermal conductivity. If other properties (*i.e.* σ and S) are maintained for single crystal NCL NWs, their ZT may be enhanced beyond the already high bulk values of 0.7–0.8.[5,9,40–42] Future work in this area will likely focus on synthesizing new thermoelectric nanowires such as Re_4Si_7, β-$FeSi_2$, and Ru_2Si_3, incorporating dopants into transition metal silicide nanowires in order to optimize their thermoelectric properties, and also exploration of the predicted effects of quantum confinement on the thermoelectric efficiency.[47,123]

Solar energy conversion

In addition to thermoelectrics, silicide nanowires are finding applications in renewable energy technologies. Specifically, devices capable of converting solar energy into electricity or chemical fuels, which are known as photovoltaic (PV) and photoelectrocatalytic (PEC) devices, respectively, will likely play a huge role in the future. Transition metal silicides, made of inexpensive and abundant elements like β-$FeSi_2$ (Si and Fe are the 2nd and 4th most abundant elements in the earth's crust, respectively) have appropriate bandgaps (0.8 eV for β-$FeSi_2$) and high light absorption coefficients,[10] and may find use in photovoltaic devices. To date there have been no reports of TMSi-based NW PV devices. This is an interesting area for future exploration. Lin and co-workers have made use of $TiSi_2$ nanonets coated with a TiO_2 layer in a PEC application.[115] In this device, $TiSi_2$ nanonets, a planar construct of orthogonal nanowire branches, act as a highly conductive scaffold and charge collection structure while a semiconducting TiO_2 layer acts as the active photoabsorption layer for water splitting (Fig. 7g). Such device configuration takes advantage of the high surface area of nanostructures to produce devices with much enhanced photocurrent compared to planar device geometry. The authors observed a peak incident photon-to-electron conversion efficiency of 16.7% using monochromatic 330 nm light. We have also synthesized highly branched and hierarchical nanostructures of other silicides such as FeSi and $MnSi_x$. These complex nanostructures could provide advantages to solar energy harvesting and conversion due to enhanced absorption and small electron-hole diffusion paths.[94]

Conclusions

In this feature article we have reviewed the current strategies for synthesizing free-standing transition metal silicide nanowires. Thus far 18 silicide NW phases across nine binary phase diagrams have been made. Even with the increasing interest in silicide NW applications, many synthetic challenges remain. For all cases besides the silicidation of silicon NWs, the mechanism for NW formation is not completely understood. Based on the reaction parameters discussed for each process, it seems plausible that silicon NWs are being formed prior to silicidation *via* metal incorporation from diffusion or directly from the gas phase. This hypothesis, if proven true, should aid in designing experiments for determining the exact mechanism for previously reported syntheses and should lead to new efforts in the synthesis of phases. Nanowires of many more interesting silicides with applications in nanoelectronics, field emission, spintronics, thermoelectrics, and solar energy conversion remain to be synthesized and exploited.

Acknowledgements

S. J. thanks Research Corporation Cottrell Scholar Award, Sloan Research Fellowship, Exxon Mobil Solid State Chemistry Fellowship, and DuPont Young Professor Grant for support. This work was also supported by an IEDR grant. J. M. H. was supported in part by a fellowship from Merck Research Laboratories.

References

1 S. L. Zhang and M. Ostling, *Crit. Rev. Solid State Mat. Sci.*, 2003, **28**, 1–129.
2 L. J. Chen, *Silicide Technology for Integrated Circuits*, The Institution of Electrical Engineers, London, UK, 2004.
3 S. L. Zhang and U. Smith, *J. Vac. Sci. Technol., A*, 2004, **22**, 1361–1370.
4 W. P. Maszara, *J. Electrochem. Soc.*, 2005, **152**, G550–G555.
5 V. E. Borisenko, *Semiconducting Silicides*, Springer, Berlin, 2000; vol. 39, p 348.
6 J. Derrien, J. Chevrier, V. Lethanh and J. E. Mahan, *Appl. Surf. Sci.*, 1992, **56–58**, 382–393.
7 D. Leong, M. Harry, K. J. Reeson and K. P. Homewood, *Nature*, 1997, **387**, 686–688.
8 M. C. Bost and J. E. Mahan, *J. Appl. Phys.*, 1988, **63**, 839–844.
9 D. M. Rowe, *CRC Handbook of Thermoelectrics*, CRC Press, Boca Raton, 1994; ch. 23–25.
10 S. Senthilarasu, R. Sathyamoorthy and S. Lalitha, *Sol. Energy Mater. Sol. Cells*, 2004, **82**, 299–305.
11 Y. Fukuzawa, T. Ootsuka, N. Otogawa, H. Abe, Y. Nakayama and Y. Makita, *Proc. SPIE–Int. Soc. Opt. Eng.*, 2006, **6197**, 61970N.
12 G. Aeppli and J. F. DiTusa, *Mater. Sci. Eng., B*, 1999, **63**, 119–124.
13 P. S. Riseborough, *Adv. Phys.*, 2000, **49**, 257–320.
14 H. Okamoto and T. B. Massalki, *Bull. Alloy Phase Diagr.*, 1983, **4**, 190–198.
15 O. Kubaschewski, in *Phase Diagrams of Binary Iron Alloys*, ed. Okamoto, H., ASM International, Materials Park, OH, 1993; pp 380–381.
16 C. Pfleiderer, D. Reznik, L. Pintschovius, H. von Lohneysen, M. Garst and A. Rosch, *Nature*, 2004, **427**, 227–231.
17 C. Pfleiderer, S. R. Julian and G. G. Lonzarich, *Nature*, 2001, **414**, 427–430.
18 Y. Ishikawa, K. Tajima, D. Bloch and M. Roth, *Solid State Commun.*, 1976, **19**, 525–528.
19 M. Uchida, Y. Onose, Y. Matsui and Y. Tokura, *Science*, 2006, **311**, 359–361.
20 N. Manyala, J. F. DiTusa, G. Aeppli and A. P. Ramirez, *Nature*, 2008, **454**, 976–980.
21 A. Neubauer, C. Pfleiderer, B. Binz, A. Rosch, R. Ritz, P. G. Niklowitz and P. Boni, *Phys. Rev. Lett.*, 2009, **102**, 186602.
22 S. Muehlbauer, B. Binz, F. Jonietz, C. Pfleiderer, A. Rosch, A. Neubauer, R. Georgii and P. Boeni, *Science*, 2009, **323**, 915–919.
23 N. Manyala, Y. Sidis, J. F. Ditusa, G. Aeppli, D. P. Young and Z. Fisk, *Nat. Mater.*, 2004, **3**, 255–262.
24 N. Manyala, Y. Sidis, J. F. DiTusa, G. Aeppli, D. P. Young and Z. Fisk, *Nature*, 2000, **404**, 581.
25 S. Pearton, *Nat. Mater.*, 2004, **3**, 203–204.
26 I. Zutic, J. Fabian and S. Das Sarma, *Rev. Mod. Phys.*, 2004, **76**, 323–410.
27 A. P. Alivisatos, *Science*, 1996, **271**, 933–937.
28 Y. Xia, P. Yang, Y. Sun, Y. Wu, B. Mayers, B. Gates, Y. Yin, F. Kim and H. Yan, *Adv. Mater.*, 2003, **15**, 353–389.
29 P. Yang, *MRS Bull.*, 2005, **30**, 85–91.
30 L. Samuelson, C. Thelander, M. T. Bjoerk, M. Borgstroem, K. Deppert, K. A. Dick, A. E. Hansen, T. Martensson, N. Panev, A. I. Persson, W. Seifert, N. Skoeld, M. W. Larsson and L. R. Wallenberg, *Physica E*, 2004, **25**, 313–318.

31 Z. L. Wang, *Annu. Rev. Phys. Chem.*, 2004, **55**, 159–196.
32 F. Wang, A. Dong, J. Sun, R. Tang, H. Yu and W. E. Buhro, *Inorg. Chem.*, 2006, **45**, 7511–7521.
33 C. N. R. Rao, F. L. Deepak, G. Gundiah and A. Govindaraj, *Prog. Solid State Chem.*, 2003, **31**, 5–147.
34 R. S. Wagner and W. C. Ellis, *Appl. Phys. Lett.*, 1964, **4**, 89–90.
35 Y. Li, F. Qian, J. Xiang and C. M. Lieber, *Mater. Today*, 2006, **9**, 18–27.
36 C. M. Lieber, *MRS Bull.*, 2003, **28**, 486–491.
37 M. Leong, V. Narayanan, D. Singh, A. Topol, V. Chan and Z. Ren, *Materials Today*, 2006, **9**, 26–31.
38 J. A. Kittl, A. Lauwers, M. A. Pawlak, M. J. H. van Dal, A. Veloso, K. G. Anil, G. Pourtois, C. Demeurisse, T. Schram, B. Brijs, M. de Potter, C. Vrancken and K. Maex, *Microelectron. Eng.*, 2005, **82**, 441–448.
39 I. Aoyama, M. I. Fedorov, V. K. Zaitsev, F. Y. Solomkin, I. S. Eremin, A. Y. Samunin, M. Mukoujima, S. Sano and T. Tsuji, *Jpn. J. Appl. Phys.*, 2005, **44**, 8562–8570.
40 V. K. Zaitsev, *Thermoelectric Properties of Anisotropic $MnSi_{1.75}$, in CRC Handbook of Thermoelectrics*, ed. Rowe, D. M., CRC Press, Boca Raton, FL, 1995; pp 299–309.
41 H. Inui, *Mater. Res. Soc. Symp. Proc.*, 2006, **886**, 219–229.
42 E. Terada, M.-W. Oh, D.-M. Wee and H. Inui, *Mater. Res. Soc. Symp. Proc.*, 2005, **842**, 425–430.
43 A. Ishida, N. L. Okamoto, K. Kishida, K. Tanaka and H. Inui, *Mater. Res. Soc. Symp. Proc.*, 2007, **980**, 235–240.
44 H. Nowotny, *Chem. Extended Defects Non-Metal. Solids, Proc. Inst. Adv. Study*, 1970, 223–237.
45 D. C. Fredrickson, S. Lee, R. Hoffmann and J. Lin, *Inorg. Chem.*, 2004, **43**, 6151–8.
46 F. E. Rohrer, H. Lind, L. Eriksson, A. K. Larsson and S. Lidin, *Z. Kristallogr.*, 2000, **215**, 650–660.
47 L. D. Hicks and M. S. Dresselhaus, *Phys. Rev. B*, 1993, **47**, 16631–4.
48 A. I. Boukai, Y. Bunimovich, J. Tahir-Kheli, J.-K. Yu, W. A. Goddard, III and J. R. Heath, *Nature*, 2008, **451**, 168–171.
49 A. I. Hochbaum, R. Chen, R. D. Delgado, W. Liang, E. C. Garnett, M. Najarian, A. Majumdar and P. Yang, *Nature*, 2008, **451**, 163–167.
50 M. S. Dresselhaus, G. Chen, M. Y. Tang, R. Yang, H. Lee, D. Wang, Z. Ren, J.-P. Fleurial and P. Gogna, *Adv. Mater.*, 2007, **19**, 1043–1053.
51 B. Poudel, Q. Hao, Y. Ma, Y. Lan, A. Minnich, B. Yu, X. Yan, D. Wang, A. Muto, D. Vashaee, X. Chen, J. Liu, M. S. Dresselhaus, G. Chen and Z. Ren, *Science*, 2008, **320**, 634–638.
52 A. L. Schmitt, M. J. Bierman, D. Schmeisser, F. J. Himpsel and S. Jin, *Nano Lett.*, 2006, **6**, 1617–1621.
53 A. L. Schmitt, L. Zhu, D. Schmeier, F. J. Himpsel and S. Jin, *J. Phys. Chem. B*, 2006, **110**, 18142–18146.
54 A. L. Schmitt, J. M. Higgins and S. Jin, *Nano Lett.*, 2008, **8**, 810–815.
55 J. M. Higgins, A. L. Schmitt, I. A. Guzei and S. Jin, *J. Am. Chem. Soc.*, 2008, **130**, 16086–16094.
56 J. R. Szczech, A. L. Schmitt, M. J. Bierman and S. Jin, *Chem. Mater.*, 2007, **19**, 3238–3243.
57 Y. Song, A. L. Schmitt and S. Jin, *Nano Lett.*, 2007, **7**, 965–969.
58 Y. Song and S. Jin, *Appl. Phys. Lett.*, 2007, **90**, 173122.
59 F. Wang, A. Dong, J. Sun, R. Tang, H. Yu and W. E. Buhro, *Inorg. Chem.*, 2006, **45**, 7511–7521.
60 H. Okamoto, *Desk handbook: phase diagrams for binary alloys*, ASM International, Materials Park, OH, 2000.
61 J. Ma, Y. Gu, L. Shi, L. Chen, Z. Yang and Y. Qian, *J. Alloys Compd.*, 2004, **375**, 249–252.
62 Y. Wu, J. Xiang, C. Yang, W. Lu and C. M. Lieber, *Nature*, 2004, **430**, 61–65.
63 Y. Chen, D. A. A. Ohlberg, G. Medeiros-Ribeiro, Y. A. Chang and R. S. Williams, *Appl. Phys. Lett.*, 2000, **76**, 4004–4006.
64 Z. He, D. J. Smith and P. A. Bennett, *Phys. Rev. Lett.*, 2004, **93**, 256102.
65 T. Ding, J. Song and Q. Cai, *Int. J. Mod. Phys. B*, 2007, **21**, 1799–1815.
66 K. Yamamoto, H. Kohno, S. Takeda and S. Ichikawa, *Appl. Phys. Lett.*, 2006, **89**, 083107.
67 B. Liu, Y. Wang, S. Dilts, T. S. Mayer and S. E. Mohney, *Nano Lett.*, 2007, **7**, 818–824.
68 K.-C. Lu, W.-W. Wu, H.-W. Wu, C. M. Tanner, J. P. Chang, L. J. Chen and K. N. Tu, *Nano Lett.*, 2007, **7**, 2389–2394.
69 Y.-C. Chou, W.-W. Wu, S.-L. Cheng, B.-Y. Yoo, N. Myung, L. J. Chen and K. N. Tu, *Nano Lett.*, 2008, **8**, 2194–2199.
70 Z. Liu, H. Zhang, L. Wang and D. Yang, *Nanotechnology*, 2008, **19**, 375602.
71 A. A. Kodentsov, M. J. H. Van Dal, C. Cserhati and F. J. J. Van Loo, *Sci. Cult. Ser., Mater. Sci.*, 2000, **1**, 187–218.
72 R. M. Walser and R. W. Bene, *Appl. Phys. Lett.*, 1976, **28**, 624–5.
73 A. M. Morales and C. M. Lieber, *Science*, 1998, **279**, 208–211.
74 J. L. Lensch-Falk, E. R. Hemesath, D. E. Perea and L. J. Lauhon, *J. Mater. Chem.*, 2009, **19**, 849–857.
75 J. Kim, E.-S. Lee, C.-S. Han, Y. Kang, D. Kim and W. A. Anderson, *Microelectron. Eng.*, 2008, **85**, 1709–1712.
76 J. Kim and W. A. Anderson, *Thin Solid Films*, 2005, **483**, 60–65.
77 C.-J. Kim, K. Kang, Y.-S. Woo, K.-G. Ryu, H. Moon, J.-M. Kim, D.-S. Zang and M.-H. Jo, *Adv. Mater.*, 2007, **19**, 3637–3642.
78 J. Kim, D. H. Shin, E.-S. Lee, C.-S. Han and Y. C. Park, *Appl. Phys. Lett.*, 2007, **90**, 253103.
79 X. Q. Yan, H. J. Yuan, J. X. Wang, D. F. Liu, Z. P. Zhou, Y. Gao, L. Song, L. F. Liu, W. Y. Zhou, G. Wang and S. S. Xie, *Appl. Phys. A*, 2004, **79**, 1853–1856.
80 K. Kang, S.-K. Kim, C.-J. Kim and M.-H. Jo, *Nano Lett.*, 2008, **8**, 431–436.
81 C.-Y. Lee, M.-P. Lu, K.-F. Liao, W.-W. Wu and L.-J. Chen, *Appl. Phys. Lett.*, 2008, **93**, 113109.
82 R. S. Wagner and W. C. Ellis, *Trans. Am. Inst. Min., Metall. Pet. Eng.*, 1965, **233**, 1053–1064.
83 A. N. Gleizes, *Chem. Vap. Deposition*, 2000, **6**, 155–173.
84 Y. L. Chueh, L. J. Chou, S. L. Cheng, L. J. Chen, C. J. Tsai, C. M. Hsu and S. C. Kung, *Appl. Phys. Lett.*, 2005, **87**, 223113.
85 Y.-L. Chueh, M.-T. Ko, L.-J. Chou, L.-J. Chen, C.-S. Wu and C.-D. Chen, *Nano Lett.*, 2006, **6**, 1637–1644.
86 Y. L. Chueh, L. J. Chou, S. L. Cheng, J. H. He, W. W. Wu and L. J. Chen, *Appl. Phys. Lett.*, 2005, **86**, 133112.
87 L. Ouyang, E. S. Thrall, M. M. Deshmukh and H. Park, *Adv. Mater.*, 2006, **18**, 1437–1440.
88 K. S. K. Varadwaj, K. Seo, J. In, P. Mohanty, J. Park and B. Kim, *J. Am. Chem. Soc.*, 2007, **129**, 8594–8599.
89 B. Xiang, Q. X. Wang, Z. Wang, X. Z. Zhang, L. Q. Liu, J. Xu and D. P. Yu, *Appl. Phys. Lett.*, 2005, **86**, 243103.
90 H.-K. Lin, Y.-F. Tzeng, C.-H. Wang, N.-H. Tai, I. N. Lin, C.-Y. Lee and H.-T. Chiu, *Chem. Mater.*, 2008, **20**, 2429–2431.
91 K. Seo, K. S. K. Varadwaj, P. Mohanty, S. Lee, Y. Jo, M.-H. Jung, J. Kim and B. Kim, *Nano Lett.*, 2007, **7**, 1240–1245.
92 K. Seo, K. S. K. Varadwaj, D. Cha, J. In, J. Kim, J. Park and B. Kim, *J. Phys. Chem. C*, 2007, **111**, 9072–9076.
93 J. In, K. S. K. Varadwaj, K. Seo, S. Lee, Y. Jo, M.-H. Jung, J. Kim and B. Kim, *J. Phys. Chem. C*, 2008, **112**, 4748–4752.
94 M. J. Bierman, Y. K. A. Lau and S. Jin, *Nano Lett.*, 2007, **7**, 2907–2912.
95 J. J. Nickl and J. D. Koukouss, *J. Less-Common Met.*, 1971, **23**, 73.
96 C. J. Barrelet, Y. Wu, D. C. Bell and C. M. Lieber, *J. Am. Chem. Soc.*, 2003, **125**, 11498–11499.
97 B. J. Aylett and H. M. Colquhoun, *J. Chem. Soc., Dalton Trans.*, 1977, 2058–2061.
98 I. Novak, W. Huang, L. Luo, H. H. Huang, H. G. Ang and C. E. Zybill, *Organometallics*, 1997, **16**, 1567–1572.
99 W. M. Weber, L. Geelhaar, A. P. Graham, E. Unger, G. S. Duesberg, M. Liebau, W. Pamler, C. Cheze, H. Riechert, P. Lugli and F. Kreupl, *Nano Lett.*, 2006, **6**, 2660–2666.
100 C.-Y. Lee, M.-P. Lu, K.-F. Liao, W.-F. Lee, C.-T. Huang, S.-Y. Chen and L.-J. Chen, *J. Phys. Chem. C*, 2009, **113**, 2286–2289.
101 H.-X. Zhang, J.-P. Ge, J. Wang and Y.-D. Li, *Nanotechnology*, 2006, **17**, S253–S261.
102 K. Seo, S. Lee, H. Yoon, J. In, K. S. K. Varadwaj, Y. Jo, M.-H. Jung, J. Kim and B. Kim, *ACS Nano*, 2009, **3**, 1145–1150.
103 L. Yu, Y. Ma, J. Zhu, H. Feng, Q. Wu, Y. Lu, W. Lin, H. Sang and Z. Hu, *J. Phys. Chem. C*, 2008, **112**, 5865–5868.
104 M.-H. Ham, J.-W. Lee, K.-J. Moon, J.-H. Choi and J.-M. Myoung, *J. Phys. Chem. C*, 2009, **113**, 8143–8146.
105 J. Du, P. Du, P. Hao, Y. Huang, Z. Ren, G. Han, W. Weng and G. Zhao, *J. Phys. Chem. C*, 2007, **111**, 10814–10817.
106 S. Zhou, X. Liu, Y. Lin and D. Wang, *Angew. Chem., Int. Ed.*, 2008, **47**, 7681–7684.
107 S. Zhou, X. Liu, Y. Lin and D. Wang, *Chem. Mater.*, 2009, **21**, 1023–1027.

108 A. L. Schmitt and S. Jin, *Chem. Mater.*, 2007, **19**, 126–128.
109 H. Nowotny, *Crystal Chemistry of Transition Metal Defect Silicides and Related Compounds, in Chemistry of Extended Defects in Non-Metallic Solids*, ed. Eyring, L.; O'Keeffe, M., North-Holland Publishing Company, Amsterdam, 1970; pp 223–237.
110 P. Villars; L. D. Calvert, *Pearson's Handbook of Crystallographic Data for Intermetallic Phases*, ASTM International, Newbury, OH, 1991; 2nd edn.
111 G. J. Snyder and E. S. Toberer, *Nat. Mater.*, 2008, **7**, 105–114.
112 F. A. Zwanenburg, C. E. W. M. van Rijmenam, Y. Fang, C. M. Lieber and L. P. Kouwenhoven, *Nano Lett.*, 2009, **9**, 1071–1079.
113 J. Kim Joong, D. Shindo, Y. Murakami, W. Xia, L.-J. Chou and Y.-L. Chueh, *Nano Lett.*, 2007, **7**, 2243–2247.
114 F. Zhou, J. Szczech, M. T. Pettes, A. L. Moore, S. Jin and L. Shi, *Nano Lett.*, 2007, **7**, 1649–1654.
115 Y. Lin, S. Zhou, X. Liu, S. Sheehan and D. Wang, *J. Am. Chem. Soc.*, 2009, **131**, 2772–2773.
116 C. Vining, *Thermoelectric Properties of Silicides, in CRC Handbook of Thermoelectrics*, ed. Rowe, D. M., CRC Press, Boca Raton, FL, 1995; pp 277–285.
117 S. L. Zhang and M. Ostling, *Crit. Rev. Solid State Mater. Sci.*, 2003, **28**, 1–129.
118 W. P. Maszara, *J. Electrochem. Soc.*, 2005, **152**, G550–G555.
119 N. S. Xu and S. E. Huq, *Mater. Sci. Eng., R*, 2005, **48**, 47–189.
120 S. Datta and B. Das, *Appl. Phys. Lett.*, 1990, **56**, 665–667.
121 G. Schmidt, D. Ferrand, L. W. Molenkamp, A. T. Filip and B. J. van Wees, *Phys. Rev. B*, 2000, **62**, R4790.
122 J. Guevara, V. Vildosola, J. Milano and A. M. Llois, *Phys. Rev. B*, 2004, **69**, 184422.
123 L. D. Hicks and M. S. Dresselhaus, *Phys. Rev. B*, 1993, **47**, 12727–12731.